Dexmedetomidine hydrochloride plus sufentanil citrate inhibits glucose metabolism and epithelial-mesenchymal transition in human esophageal squamous carcinoma KYSE30 cells by modulating the JAK/STAT3/HIF-1α axis

WEIJING LI[1], YONG WANG[1], XIAOLIN LI[2], HAN WU[1] and LI JIA[1]

[1]Department of Anesthesiology, The Fourth Hospital of Hebei Medical University, Shijiazhuang, Hebei 050011; [2]Department of Anesthesiology, The Second Hospital of Hebei Medical University, Shijiazhuang, Hebei 050000, P.R. China

Received July 3, 2023; Accepted November 10, 2023

DOI: 10.3892/ol.2024.14406

Abstract. Dexmedetomidine hydrochloride (DEX-HCl) and sufentanil citrate (SFC) are commonly used anesthetic drugs for esophageal cancer (EC) surgery. The present study was performed to investigate the effect of DEX-HCl and SFC treatment on glucose metabolism and epithelial-mesenchymal transition in EC. Cell counting kit-8 (CCK8), clonogenic, wound healing and Transwell migration assays were performed to assess the effects of the DEX-HCl and SFC on KYSE30 cell proliferation, invasion and migration. Changes in lactate and glucose levels in KYSE30 cells were also detected. Western blot analysis was used to determine the protein expression levels of the JAK/STAT signaling pathway and glucose metabolism-related proteins. The results of CCK8, clonogenic and wound healing assays demonstrated that DEX-HCl and SFC inhibited KYSE30 cell proliferation, invasion and migration. Similarly, the combined DEX-HCl and SFC treatment significantly reduced lactate production, ATP production and glucose levels in KYSE30 cells. Western blotting indicated that DEX-HCl and SFC could reduce JAK/STAT and metastasis-related protein expression. Demonstrating a reduction in Hexokinase 2, matrix metallopeptidase 2 and 9, N-cadherin and lactate dehydrogenase A protein expression levels. The effects of DEX-HCl and SFC combined treatment were counteracted by the addition of JAK/STAT pathway activator RO8191, which suggested that DEX-HCl and SFC could serve a role in mediating the JAK/STAT signaling pathway in KYSE30 cells.

Correspondence to: Professor Han Wu or Professor Li Jia, Department of Anesthesiology, The Fourth Hospital of Hebei Medical University, 12 Jiankang Road, Shijiazhuang, Hebei 050011, P.R. China
E-mail: hxg820602@126.com
E-mail: jiali070825@163.com

Key words: dexmedetomidine hydrochloride, sufentanil citrate, glucose metabolism, invasion

Introduction

Esophageal cancer (EC) is a complex and common cancer with a highly aggressive nature (1). Esophageal squamous cell carcinoma (ESCC), a malignant epithelial tumor originating from EC (2), is one of the most common subtypes of EC, which typically presents as progressive dysphagia. In 2020, there were 604,000 new cases and 544,000 deaths from esophageal cancer worldwide. By 2040, these numbers are expected to increase to 957,000 cases and 880,000 deaths per year (3), constituting a serious public health issue. The pathogenesis of EC is associated with dietary habits, environmental factors, geographic location and gender (4). EC has a 5-year overall survival rate of 15-25% in developing countries and is the sixth leading cause of cancer-associated mortalities in men worldwide (5). Furthermore, the rates of EC mortality and morbidity are higher in developing countries compared with in developed countries (6). Clinically, esophageal carcinoma is typically managed by drug therapy, surgery, radiotherapy and chemotherapy. However, side effects originating from these therapies and the poor prognosis of patients remain a major concern, creating an urgent need to evaluate new treatment modalities and improve the treatment and prognosis of patients with EC (7).

Epithelial mesenchymal transformation (EMT) is a process in which epithelial cells lose their cell polarity, lose their connection to the basement membrane and gain a higher interstitial phenotype such as migration and invasion, anti-apoptosis, and degradation of the extracellular matrix (8). According to the literature, EMT progression will reduce the adhesion capacity of tumor cells, make them more invasive and migratory, and accelerate tumor cell invasion and metastasis (9). This also suggests that the inhibition of the EMT process could hinder the metastasis of cancer cells. In addition, cancer cells need a large amount of energy to support the process of metastasis, and the abnormal glucose metabolism of tumor cells can support this requirement, assisting cancer cells in metastasis (10). Abnormal glucose metabolism is one of the major changes seen in the tumor microenvironment (11). Thus, glucose metabolism-related gene regulation has emerged as a new target for tumor therapy. The Janus kinase (JAK)/signal transducer and activator (STAT) signaling

pathway is a ubiquitously expressed intracellular signal transduction pathway that is involved in a number of key biological processes, including cell proliferation, differentiation, apoptosis and immune regulation (12). Studies have reported that JAK/STAT signaling pathway can regulate the glycolytic pathway in lung cancer (13), renal cell carcinoma (14) and breast cancer (15) cells, and so have the potential to modulate cancer progression. Furthermore, high expression of phosphorylated (p)-JAK1 and p-STAT3 indicates poor prognosis in patients with EC (16). Zhao *et al* (17) reported that STAT3 and hypoxia-inducible factor-1α (HIF-1α) were both expressed at higher levels in ESCC tissues than in normal tissues, and the addition of JAK2 inhibitors was effective in blocking the proliferation of EC cells *in vitro* (18). It was also reported that the inhibition of the JAK/STAT signaling pathway blocked the angiogenesis of EC cells (19). Accordingly, this evidence suggests that inhibition of the JAK/STAT signaling pathway is a potential target for the treatment of EC. Hexokinase (HK)1 and HK2 are the two major HKs and depletion of HK2 has been reported to reduce lactate and cellular HK activity. The depletion of HK1 contributes little to the proliferative activity of these cells, and the alteration of HK1 has a less significant effect on lactate content compared with HK2. The role of HK2 in tumor glucose metabolism is now widely reported (20,21). Therefore, the present study focused on HK2.

Furthermore, studies have shown that dexmedetomidine hydrochloride (DEX-HCl) alleviated neuropathic pain by modulating the JAK/STAT signaling pathway (22) and prevented reperfusion injury (23,24). During surgery in patients with cancer, anesthetic drugs may affect the growth, proliferation and metastasis of cancer cells (25,26). However, these findings require further clinical trials and validation, and currently it is not possible to determine whether the effects of anesthetic drugs on cancer cells have clinical application value. In order to further investigate the specific effects of anesthetics on cancer cells, the present study investigated the effects of DEX-HCl and sufentanil citrate (SFC) on the JAK/STAT signaling pathway, and evaluated their effects on the glucose metabolism, lactic acid production, ATP level, invasion and migration of EC KYSE30 cells. This may provide a theoretical basis for clinical cancer-associated anesthesia.

Materials and methods

Cell culture. Human ESCC cell lines KYSE30, KYSE520, KYSE140 and KYSE410 and immortalized HEEC human normal esophageal epithelial cells were purchased from the Qingqi (Shanghai) Biotechnology Development Co., Ltd. The cells were cultured in RPMI-1640 medium (Gibco; Thermo Fisher Scientific, Inc.) containing 10% fetal bovine serum (Shanghai ExCell Biology, Inc.) and 1% penicillin-streptomycin mixture (Beijing Solarbio Science & Technology Co., Ltd.) in a 37˚C, 5% CO_2 incubator (Zhejiang Jiemei Electronic & Technology Co., Ltd.). The medium was changed every two days and cells were allowed to grow to the exponential phase for use in subsequent experiments.

Cell counting kit-8 assay. KYSE30 cells at exponential culture stage were taken out of the cell incubator. The medium was discarded and the cells were washed with PBS three times. Digestion was performed in T25 culture flasks by adding 1 ml of trypsin solution (Beijing Solarbio Science & Technology Co., Ltd.) for 2-3 min. Subsequently, 2 ml of RPMI-1640 complete medium was added to terminate the digestion. The cells were collected in a centrifuge tube and centrifuged at 1,200 x g for 3 min. RPMI-1640 complete medium was added to resuspend the cells, and 10 μl of cell suspension was aspirated to count the number of cells using a cell counter (Countess™ 3; cat. no. AMQAX2000; Invitrogen; Thermo Fisher Scientific, Inc.). The cells were transferred to 96-well plates at a concentration of 3,000 cells per well and incubated overnight in a cell incubator at 37˚C and divided into four groups which were treated as follows: i) Control (DMSO); ii) DEX-HCl (25, 50, 100 and 200 nmol/l); iii) SFC (1.25, 2.5, 5 and 10 μmol/l); and iv) DEX-HCl (25 nmol/l) and SFC (1.25 μmol/l) combined treatment. The 96-well plate was then incubated for 48 h. A total of 10 μl of CCK-8 solution (Beijing Solarbio Science & Technology Co., Ltd.) was added to each well and incubated for 3 h. The absorbance at 450 nm was measured using an enzyme immunoassay analyzer (ReadMax 1,200; Shanghai Shanpu Biotechnology Co., Ltd.). IC_{50} values were calculated using GraphPad Prism 9.5.0 (Dotmatics). DEX-HCI (cat. no. 22022431) was purchased from Jiangsu Hengrui Pharmaceutical Co., Ltd., and SFC (cat. no. 21A09311) was purchased from Yichang Renfu Pharmaceutical Co., Ltd.

Clonogenic assay of cells in vitro. KYSE30 cells at the exponential growth phase were subjected to cell digestion and cell counting as described previously for the CCK-8 assay. The cells were resuspended at 150 cells/ml. A total of 1 ml of cell suspension was mixed with 1 ml of RPMI-1640 complete medium, transferred to a six-well plate and incubated overnight in an incubator at 37˚C with 5% CO_2. The medium was replenished every 2 days for 14 days. The medium was then discarded, the cells were rinsed with PBS solution three times and then stained using 0.1% crystal violet (Beijing Solarbio Science & Technology Co., Ltd.) for 15 min, 25˚C. The cells were washed three times with PBS, air-dried naturally and imaged with an SLR camera (Nikon D850; Nikon Corporation). The images were analyzed using ImageJ version 1.52a (National Institutes of Health) bundled with Java 8.

Wound healing assay. KYSE30 cells at the exponential growth phase were subjected to cell digestion and cell counting as described previously for the CCK-8 assay. The cell suspension was inoculated into 6-well plates at $5x10^5$ cells per well and incubated overnight in a cell culture incubator (37˚C and 5% CO_2). Three parallel vertical lines were drawn across the bottom of the six-well plate with a 10 μl pipette tip. After discarding the medium, the cells were washed three times with PBS, and serum-free RPMI-1640 medium containing DEX-HCl (25 nmol/l) and SFC (1.25 μmol/l) drug solution was added to a 6-well plate and incubated in an incubator. The six-well plate was imaged at 0, 24 and 48 h using an inverted fluorescence microscope [Sunny Optical Technology (Group) Co., Ltd.] at the intersection of the horizontal and vertical lines to ensure that images were obtained from the same location at different time points. The cell migration rate of each group was analyzed by ImageJ version 1.52a (National Institutes of Health) bundled with Java 8.

Transwell migration assay. Matrix-Gel™ Matrigel (cat. no. C0371; Beyotime Institute of Biotechnology) was diluted 1:8 with serum-free RPMI-1640 medium and spread on the upper part of the Transwell chamber, and then left to set at 37˚C for 2 h. Culture medium was then added to hydrate the gel for 30 min before being discarded. KYSE30 cells at the exponential phase were collected and counted as described previously. The cell concentration was diluted to $1x10^6$ cells/ml with serum-free RPMI-1640 medium and 50 μl of cell suspension was added to the upper chamber of the Transwell. The upper chamber of the Transwell was supplemented with 50 μl of serum-free RPMI 1640 medium containing DEX-HCl and SFC to give a final drug concentration of 25 nmol/l DEX-HCl and 1.25 μmol/l SFC. 500 ul of RPMI 1640 medium containing 20% FBS was added to the lower chamber of the Transwell. The Transwell chambers were then incubated in a cell culture incubator at 37˚C for 12 h. Subsequently, 500 μl of cell fixation solution (cat. no. P0099; Beyotime Institute of Biotechnology) was added to each chamber for 25 min at room temperature, then washed with PBS. Finally, the cells were stained with 0.1% crystal violet solution for 25 min at room temperature before being imaged using a microscope.

Glucose, lactate and ATP content assay. After adding DEX-HCI (25 nmol/l) or SFC (1.25 μmol/l) alone or in combination, KYSE30 cells were incubated in a cell incubator at 37˚C for 24 h. Cells were then collected and transferred to a 1.5 ml centrifuge tube with a sterile cell scraper. Cells were resuspended in 1 ml of distilled water and sonicated (cat. no. E0380; Beyotime Institute of Biotechnology) at room temperature for 1 min (40 Hz; ultrasound for 5 sec followed by 5 sec pauses). The cell lysate was incubated for 10 min in a water bath at 4˚C and centrifuged at 12,000 x g for 15 min. The experiments were carried out according to the manufacturer's protocols of each kit using a UV spectrophotometer (Cary 60 UV-Vis; Agilent Technologies, Inc.) to determine the ATP, lactate and glucose content. ATP (cat. no. S0026), glucose (cat. no. S0201S) and lactate (cat. no. C0016) kits were purchased from Beyotime Institute of Biotechnology.

Immunofluorescence. The RO8191 reverse validation experiment was divided into four groups and were treated as follows: i) Control (DMSO); ii) RO8191 (1 μmol/l); iii) DEX-HCl (25 μmol/l) combined with SFC (1.25 μmol/l); and iv) combined treatment with DEX-HCl (25 μmol/l), SFC (1.25 μmol/l) and RO8191 (1 μmol/l). Different drugs were added to KYSE30 cells according to the requirements of the different groups, and the cells were incubated in a cell incubator at 37˚C for 48 h, the cells were digested, centrifuged and resuspended as previously described. The cell samples were incubated with 4% paraformaldehyde at room temperature for 20 min, then incubated with 0.5% Triton X-100 for 20 min. Subsequently, 5% bovine serum albumin (cat. no. SW3015; Beijing Solarbio Science & Technology Co., Ltd.) was added and the cells were incubated for 1 h at room temperature. The samples were incubated with primary antibodies at 4˚C overnight and the cells were then washed with 1% Tween TBST for 3 min. The primary antibodies used were: E-cadherin (cat. no. ET1607-75; 1:100) and N-cadherin (cat. no. ET1607-37; 1:100), which were purchased from Hangzhou HuaAn Biotechnology Co., Ltd. Fluorescently labeled secondary antibodies (cat. no. ZF-0511; 1:500; Beijing Zhongshan Jinqiao Biotechnology Co., Ltd.) were added and incubated in the dark at room temperature for 1 h. The slides were incubated with DAPI in the dark for 5 min, sealed with an anti-fluorescence quencher (cat. no. P0131; Beyotime Institute of Biotechnology), imaged using a confocal microscope and analyzed using ImageJ version 1.52a (National Institutes of Health) bundled with Java 8.

Reverse transcription-quantitative (RT-q)PCR. After treating KYSE30 cells with DEX-HCI (25 nmol/l) or SFC (1.25 μmol/l) alone or in combination for 24 h, the cells were collected with a sterile cell scraper and transferred to a 1.5 ml centrifuge tube. The RNA was extracted using TRIzol (Beijing Solarbio Science & Technology Co., Ltd.), according to the manufacturer's instructions. Briefly, cells were resuspended in 1 ml of TRIzol and incubated at room temperature for 5 min. The RNA sample was used immediately or stored at -80˚C. RNA concentration was measured using a Q5000 UV-Vis Spectrophotometer (Pono-550; Prebo Instruments (Hangzhou) Co., Ltd.). RNA was reverse transcribed (at 42˚C for 15 min) using the FastKing gDNA Dispelling RT SuperMix kit (Tiangen Biotech Co., Ltd.). The reverse transcribed complementary DNA (cDNA) was used immediately or stored in at -80˚C. The cDNA concentration was measured using a Dalong Gradient Thermal Cycler TC1000-G (Shaying Scientific Instruments (Shanghai) Co., Ltd.) and amplified in a CFX Connect Real-Time PCR Detection System (Bio-Rad Laboratories, Inc.,) using FastKing One Step RT-qPCR kit (SYBR Green) (Tiangen Biotech Co., Ltd.). The primers used for RT-qPCR are listed in Table I. The thermal cycling conditions used were: 50˚C for 30 min; 95˚C for 3 min; followed by 40 cycles of 95˚C for 15 s and 60˚C for 30 s. By comparing the target gene Cq with the internal reference Cq, ΔCq for each group, and the fold difference was calculated by $2^{-\Delta\Delta Cq}$ (27). GraphPad Prism version 9.5.0 (Dotmatics) was used for statistical analysis.

Western blotting. DEX-HC (25 nmol/l), SFC (1.25 μmol/l) and RO819 (1 μmol/l) were added to KYSE30 cells according to the aforementioned grouping requirements and incubated in a cell incubator at 37˚C for 48 h. The cells were then digested and centrifuged according to the aforementioned method. The RIPA solution (cat. no. R0010; Beijing Solarbio Science & Technology Co., Ltd.) was added to the cell precipitate and incubated on ice for 30 min. The lysate was cleared by centrifugation at 12,000 x g for 10 min at 4˚C. Protein quantification was performed with bicinchoninic acid (BCA) protein quantification kit. Protein samples (30 μg) were loaded on a 10% polyacrylamide gel and separated by SDS-PAGE for 35 min at 80 V, then 120 V for 60 min. Proteins were transferred to a PVDF membrane using the Trans-Blot® Turbo™ Transfer System (Bio-Rad Laboratories, Inc.) for 1 h, with a constant current of 260 mA. The PVDF membrane was blocked using 5% skimmed milk powder for 2 h at room temperature, and then washed with TBST (0.1% Tween) for 30 min. The membrane was then incubated with the corresponding primary antibodies at 4˚C overnight. The PVDF membrane was washed 3 times with TBST (0.1% Tween) for 30 min, then blocked with 5% skim milk powder and

Table I. Sequences of primers used for reverse transcription-quantitative PCR.

Gene	Primer (5'-3')
HIF-1α	F: GAACGTCGAAAAGAAAAGTCTCG
	R: CCTTATCAAGATGCGAACTCACA
HK2	F: GTGAATCGGAGAGGTCCCAC
	R: GCTAACTTCGGCCACAGGAT
LDHA	F: CTGGCTGTGTCCTTGCTGTA
	R: TCACGTTACGCTGGACCAAA
GAPDH	F: GATTCCACCCATGGCAAATTC
	R: CTGGAAGATGGTGATGGGATT

HIF-1α, hypoxia inducible factor 1α; HK2; hexokinase II; LDHA lactate dehydrogenase A; F, forward; R, reverse.

incubated with secondary antibodies for 1 h at room temperature. Images were processed and analyzed using ImageJ version 1.52a (National Institutes of Health) bundled with Java 8. Antibodies used were as follows: β-actin (cat. no. EM21002; HUABIO; 1:2,000), anti-JAK2 (cat. no. M1501-8; HUABIO; 1:1,000), p-JAK2 (cat. no. ET1607-34; HUABIO; 1:1,000), STAT3 (cat. no. ET1607-38; HUABIO; 1:1,000), p-STAT3 (cat. no. ET1603-40; HUABIO; 1:1,000), HIF-1α (cat. no. R1510-5; HUABIO; 1:1,000), MMP2 (cat. no. bs-4605R; BIOSS; 1:1,000), MMP9 (cat. no. bs-4593R; BIOSS; 1:1,000), E-cadherin (cat. no. ET1607-75; Hangzhou HuaAn Biotechnology Co., Ltd.; 1:100), N-cadherin (cat. no. ET1607-37; Hangzhou HuaAn Biotechnology Co., Ltd.; 1:100), HK2 (cat. no. A0994; ABclonal Biotech Co., Ltd.; 1:1,000), lactate dehydrogenase A (LDHA; cat. no. A1146; ABclonal Biotech Co., Ltd.; 1:1,000), HRP Goat anti-rabbit (cat. no. AS014; ABclonal Biotech Co., Ltd.; 1:10,000) and HRP Goat anti-mouse (cat. no. AS003; ABclonal Biotech Co., Ltd.; 1:10,000).

Statistical analysis. Statistical analysis was performed using SPSS 22.0 software (IBM Corp.). Measurement data are presented as mean ± standard deviation. All data were analyzed using one-way ANOVA, followed by Tukey's post hoc analysis. All parallel experiments were repeated three or more times. $P<0.05$ was considered to indicate a statistically significant difference.

Results

DEX-HCl and SFC inhibit KYSE30 cell proliferation. The relative molecular masses and structural formula of DEX-HCI and SFC are presented in Fig. 1A and B. Among the four esophageal squamous cell carcinoma cell lines (KYSE30, KYSE520, KYSE140 and KYSE410), p-STAT 3 and p-JAK were more significantly up-regulated in KYSE30 cells compared with normal human esophageal epithelial HEEC, and thus KYSE30 was chosen for use in further experiments (Fig. S1). CCK-8 and clonogenic assays of KYSE30 cells treated with DEX-HCl (25, 50, 100 and 200 nmol/l) and SFC (1.25, 2.5, 5 and 10 μmol/l) *in vitro* showed a significant and concentration-dependent decrease in cell viability compared with the control group after 48 h of treatment (Fig. 1C and D). Compared with DEX-HCL or SFC alone, the combination treatment demonstrated enhanced inhibition of KYSE30 cell viability (Fig. 1E). The IC_{50} was calculated to be 83.96 nmol/l for DEX-HCl and 2.173 μmol/l for SFC. In subsequent experiments concentrations $<IC_{50}$ values were used, and thus, DEX-HCl was used at 25 nmol/l and SFC was used at 1.25 μmol/l. To evaluate the effect of the co-administration of DEX-HCl and SFC, the technique previously described by Chou (28) was used. The combination index (CI) theory provides quantitative definitions of additive effect (CI, 1), synergistic effect (CI, <1) and antagonistic effect (CI, >1) in drug combinations. The smaller the value of CI, the stronger the synergistic effect of drugs. The CI of DEX-HCl and SFC was 0.27, demonstrating a strong synergistic effect between DEX-HCl and SFC (Fig. 1E). The results of the clonogenic assay demonstrated that DEX-HCl and SFC were able to inhibit the proliferation of KYSE30 cells and demonstrated enhanced inhibition of KYSE30 cells in combination compared with single dosing, which suggested that DEX-HCl and SFC were more effective in combination (Fig. 1F and G).

Effects of DEX-HCl and SFC on the invasion and migration ability of KYSE30 cells. Wound healing and Transwell assays were performed to assess the effects of DEX-HCl and SFC on cell migration and invasion. The wound healing assay results demonstrated that KYSE30 cells treated with DEX-HCl (25 nmol/l) or SFC (1.25 μmol/l) for 24 and 48 h demonstrated an inhibited migration, and demonstrated a significantly greater inhibition after co-administration for both 24 and 48 h after treatment. Cells that were treated with DEX-HCl and SFC in combination only healed 10% after 24 h of treatment, as shown in Fig 2A. The wound healing assay results demonstrated that DEX-HCI and SFC had an inhibitory effect on cell migration, while the DEX-HCI combined with SFC group had a stronger inhibitory effect on cell migration compared with the DEX-HCI (25 nmol/l) or SFC (1.25 μmol/l) only groups. In the DEX-HCI + SFC group there was also a time-dependent effect, and the longer the migration time, the stronger the inhibition ability of migration (Fig. 2A). The Transwell migration assay demonstrated that the cell invasion ability of KYSE30 cells treated with DEX-HCl (25 nmol/l) or SFC (1.25 μmol/l) was significantly inhibited after 12 h compared with the control group. The combination of DEX-HCl and SFC significantly increased the inhibitory effect on the invasive ability of KYSE30 cells compared with the single treatment groups (Fig. 2B).

DEX-HCl and SFC reduce glucose metabolism in KYSE30 cells. Changes were observed in ATP levels, lactate production and glucose uptake in KYSE30 cells after treatment with DEX-HCl and SFC. The results showed that ATP levels, lactate production and glucose uptake were significantly reduced in KYSE30 cells in the DEX-HCl group, SFC group and the combination group compared with the control group (Fig. 2C). The combination group showed significantly decreased ATP levels, lactate production and glucose uptake in KYSE30 cells compared with the DEX-HCl and SFC alone groups (Fig. 2C).

DEX-HCl and SFC impact protein expression in KYSE30 cells. To investigate the mechanism of action, the expression

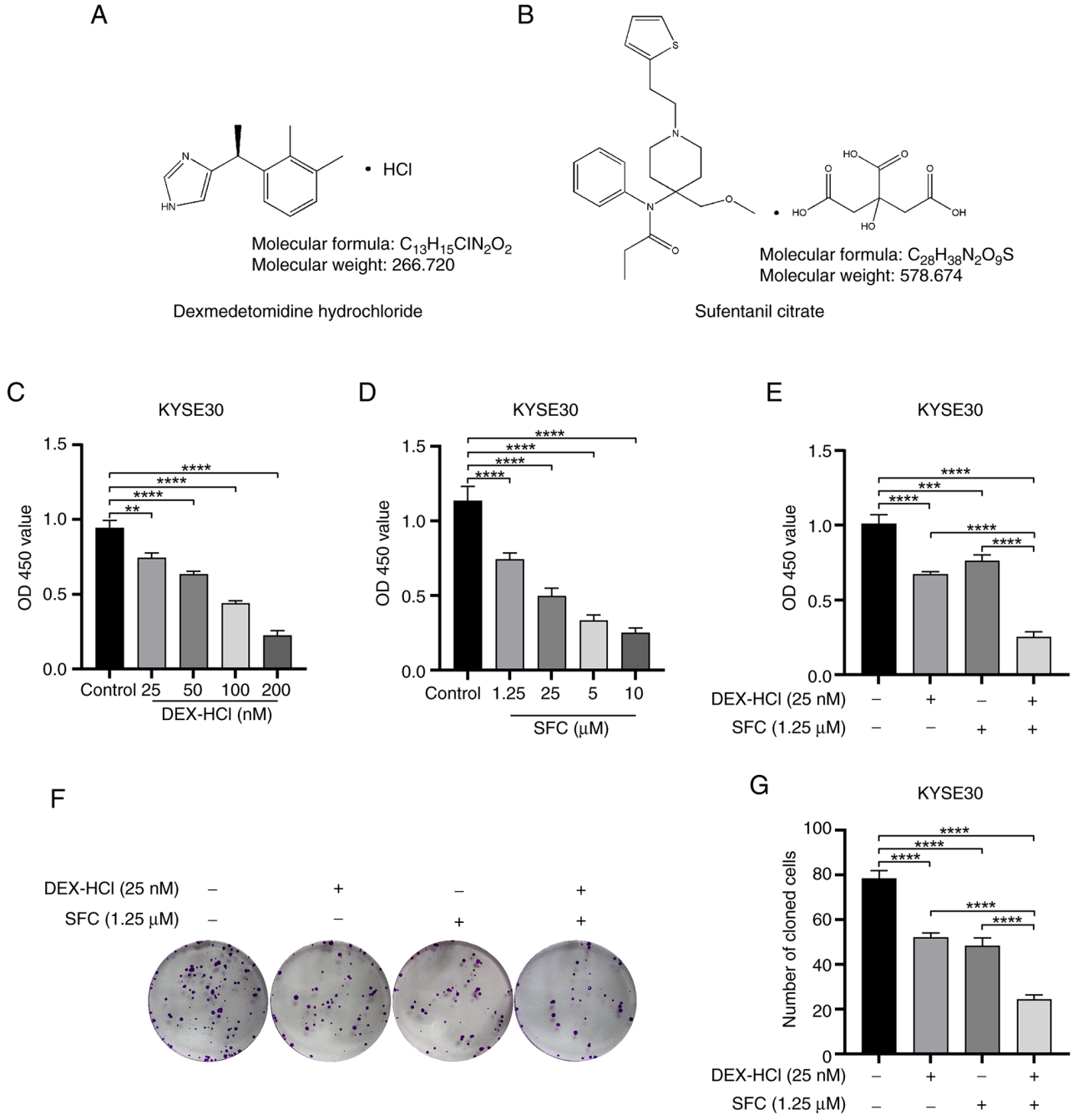

Figure 1. DEX-HCl and SFC inhibit the proliferation of KYSE30 cells. Molecular structure, formula and relative molecular mass of (A) DEX-HCl and (B) SFC. (C) CCK8 assay to examine the effect of DEX-HCl on the proliferation of KYSE30 cells. (D) CCK8 assay to examine the effect of SFC on KYSE30 cell proliferation. (E) Effect of DEX-HCl and SFC combined treatment on KYSE30 cell proliferation. (F) Clonogenic assay of cells *in vitro* to detect the effect of DEX-HCl and SFC combined treatment on cell proliferation. (G) Histogram of the number of cells with clonogenic capacity. **P<0.01, ***P<0.001, ****P<0.0001. DEX-HCl, Dexmedetomidine hydrochloride; SFC, sufentanil citrate; CCK8, cell counting kit 8.

of JAK/STAT3/HIF-1α pathway-related, invasion-related marker proteins and glycolysis-related marker proteins were assessed using qPCR and western blotting. The results of the qPCR and western blotting experiments demonstrated that both DEX-HCI and SFC were able to significantly reduce the expression and protein levels of HIF-1α, HK2 and LDHA. Additionally, the combination group of DEX-HCI and SCF inhibited the expression and protein levels of HIF-1α, HK2 and LDHA more strongly compared with that of the drug alone (Fig. 3A and B). It was also demonstrated that DEX-HCl and SFC treatment significantly decreased the protein expression levels of p-STAT3 and p-JAK compared with the control group. The co-administration of DEX-HCl and SFC demonstrated a further significant decrease in the protein expression levels of p-STAT3 and p-JAK compared with both the control and single treatment groups alone (Fig. 3C), without affecting the expression levels of STAT3 and JAK proteins. The protein expression levels of E-cadherin and N-cadherin were examined by immunofluorescence assay and western blotting and the results showed that DEX-HCl and SFC were able to significantly upregulate E-cadherin and significantly downregulate N-cadherin protein expression compared with the negative

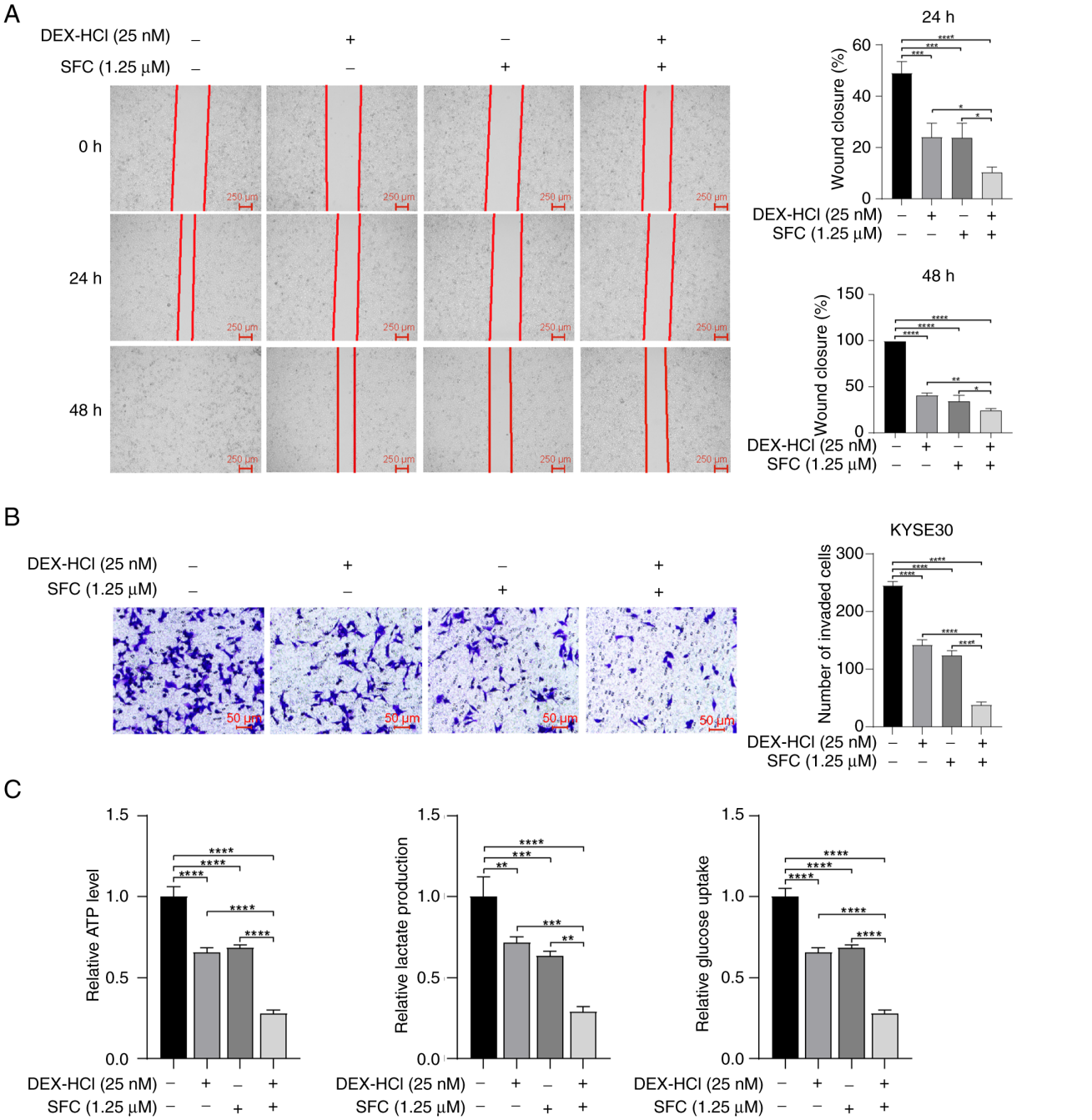

Figure 2. DEX-HCl and SFC inhibit the invasion, migration and glucose metabolism of KYSE30 cells. (A) Wound healing assay to detect the effect of DEX-HCl combined with SFC on KYSE30 cell migration. (B) Transwell assay to detect the effect of DEX-HCl combined with SFC on KYSE30 cell invasion. (C) Detection of changes in lactate, glucose and ATP content in KYSE30 cells. *P<0.05, **P<0.01, ***P<0.001, ****P<0.0001. DEX-HCl, Dexmedetomidine hydrochloride; SFC, sufentanil citrate.

control in KYSE30 cells. SFC significantly reduced the expression levels of MMP2 and MMP9 proteins in KYSE30 cells. DEX-HCI significantly reduced the protein expression level of MMP9, but the addition of DEX-HCI could not significantly reduce the protein expression level of MMP2. The DEX-HCI + SFC group significantly reduced the expression level of the MMP2 protein compared with the DEX-HCI group and SFC group, which further indicated that DEX-HCI and SFC combined have a drug synergistic effect (Fig. 4A and B).

DEX-HCI combined with SFC inhibited the invasion of KYSE30 cells by inhibiting the JAK/STAT3/HIF-1α pathway. To further assess whether DEX-HCl and SFC effect KYSE30 cell glucose metabolism and invasion through the JAK/STAT3/HIF-1α axis, reverse validation experiments were performed by adding RO8191 to induce STAT3/JAK to undergo phosphorylation.

RO8191 is an imidazolino pyridine compound that activates phosphorylation of JAK and STAT proteins thereby activating the JAK/STAT signaling pathway (29). Therefore, recovery of the invasion and migration ability of KYSE30 with the addition of RO8191 would suggest that DEX-HCl and SFC exhibit their function via the JAK/STAT pathway. The addition of RO8191 in the Transwell migration assay counteracted

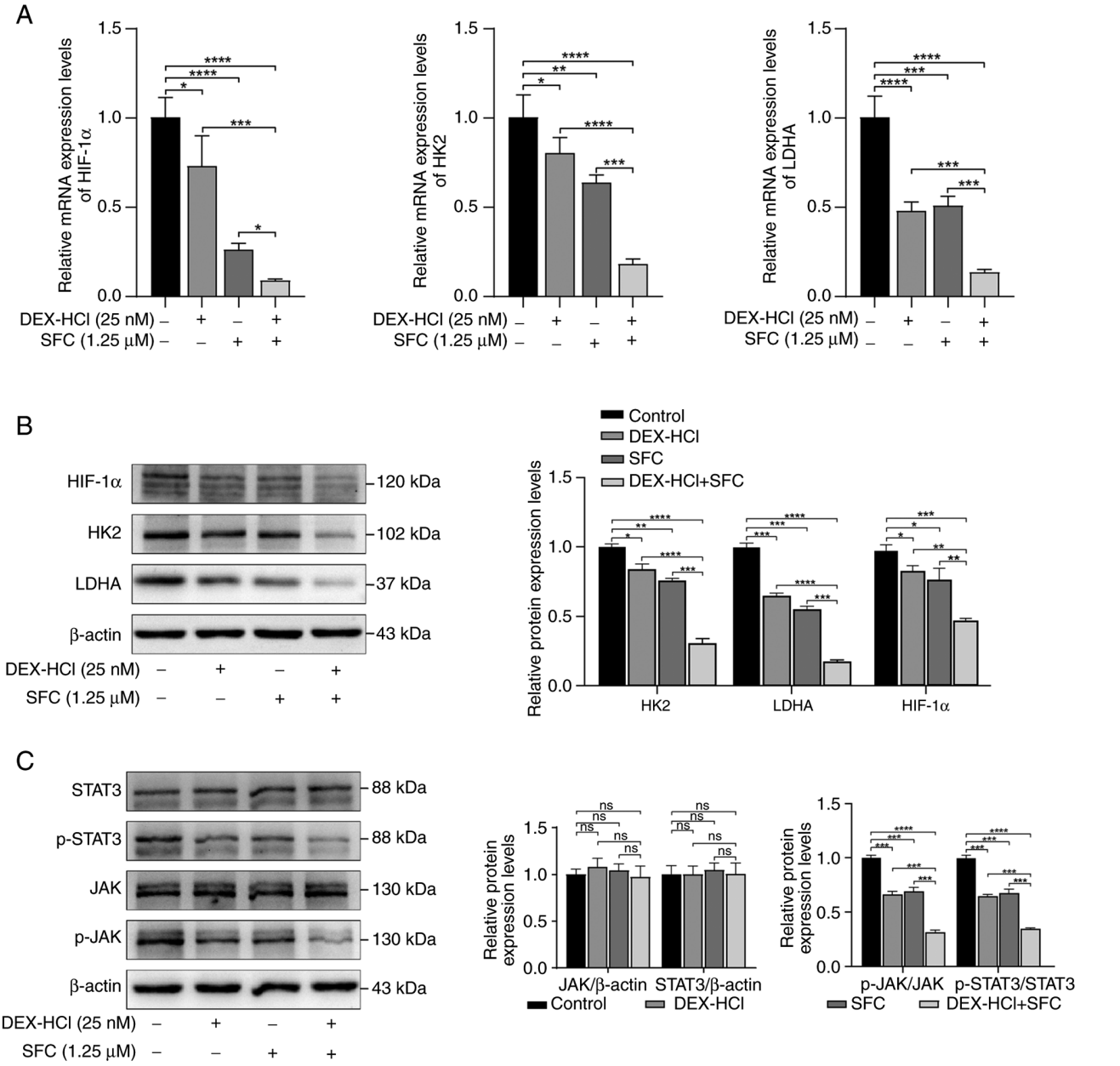

Figure 3. Effect of DEX-HCl and SFC on glucose metabolism and JAK/STAT pathway-related protein expression in KYSE30 cells. (A) RT-qPCR assay to detect changes in relative mRNA expression of HIF-1α, HK2, and LDHA genes in KYSE30 cells. (B) Semi-quantified protein expression levels assessed by western blotting of HK2, LDHA and HIF-1α in KYSE30 cells. (C) Semi-quantified protein expression levels assessed by western blotting of STAT3, p-STAT3, JAK and p-JAK in KYSE30 cells. *P<0.05, **P<0.01, ***P<0.001, ****P<0.0001; ns, not significant (P>0.05). DEX-HCl, Dexmedetomidine hydrochloride; SFC, sufentanil citrate; RT-qPCR, reverse transcription quantitative PCR.

the inhibitory effect of DEX-HCl and SFC treatment on KYSE30 cells, significantly increasing the number of invaded cells compared with the DEX-HCl and SFC treatment group (Fig. 5A). DEX-HCL combined with SFC was demonstrated to reduce the expression levels of HIF-1α, HK2 and LDHA mRNA, whereas the addition of RO8191 was demonstrated to upregulate the expression levels of HIF-1α, HK2 and LDHA mRNA, counteracting the inhibitory effect of DEX-HCL combined with SFC (Fig. 5B).

Glucose uptake, ATP levels and lactate production of KEYSE30 cells significantly increased after treatment with RO8191 compared with the DEX-HCl and SFC co-administration group (Fig. 5C). DEX-HCI combined with SFC significantly inhibited the expression levels of HK2, LDHA, p-JAK, p-STAT3, and HIF-1α proteins, whereas RO8191 co-administration increased the expression levels of HK2, LDHA, p-JAK, p-STAT3 and HIF-1α proteins, counteracting the effect of DEX-HCI combined with SFC (Fig. 5D and E). Likewise, the addition of RO8191 in immunofluorescence experiments showed a significant decrease in E-cadherin fluorescence intensity compared with the DEX-HCl and SFC treatment group and a significant increase in N-cadherin fluorescence compared with the DEX-HCl and SFC treatment group (Fig. 6A). The addition of RO8191 was also demonstrated to increase the protein expression levels of MMP2, MMP9 and N-cadherin and decrease the protein expression levels of E-cadherin compared with the DEX-HCl and SFC treatment group (Fig. 6B). In summary, DEX-HCI

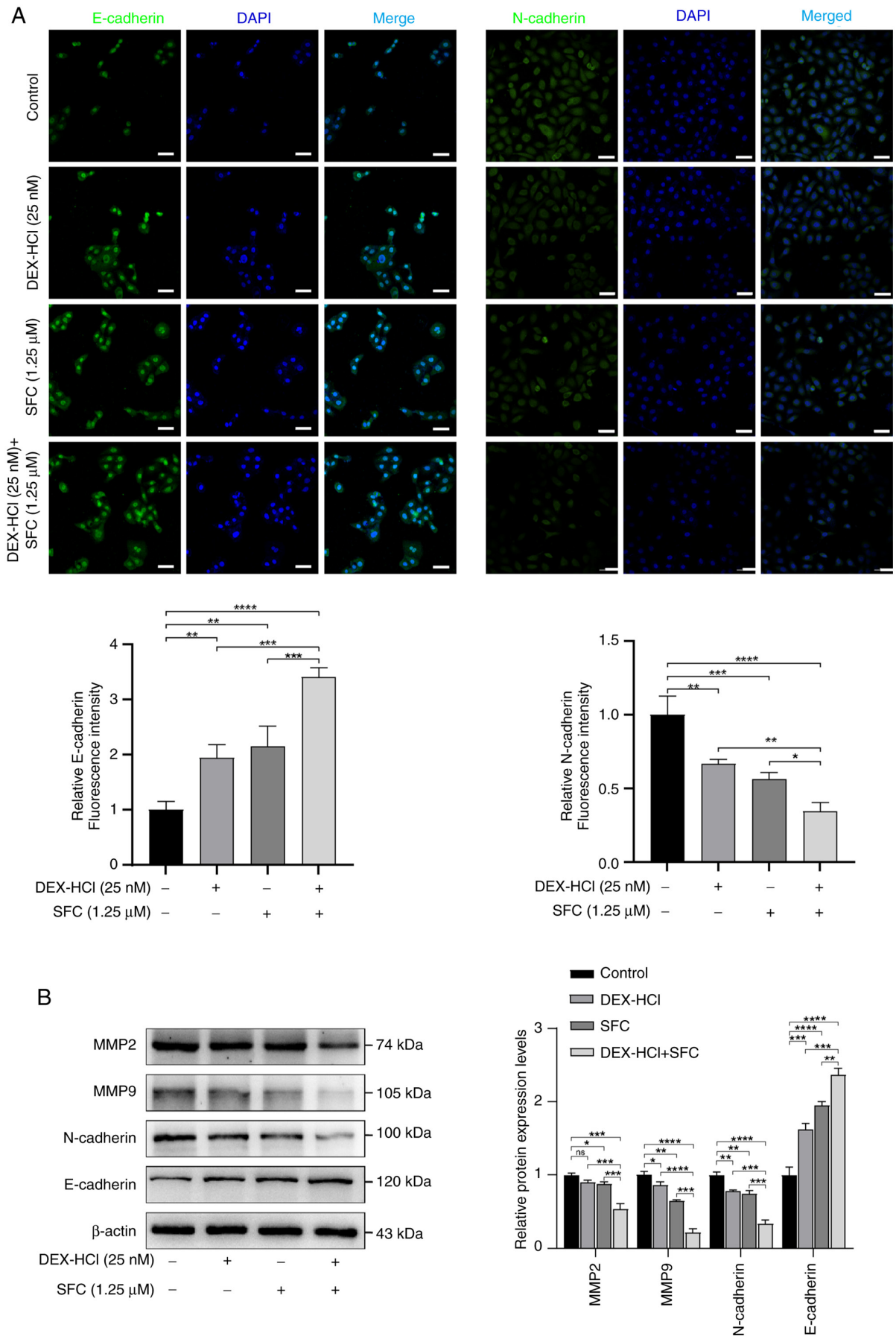

Figure 4. Effects of DEX-HCl in combination with SFC on invasion-related proteins. (A) The expression of the invasion-associated proteins E-cadherin and N-cadherin was determined by immunofluorescence (scale bar, 50 μm). (B) Semi-quantified protein expression levels assessed by western blotting of MMP 2, MMP 9, E-cadherin and N-cadherin. *P<0.05, **P<0.01, ***P<0.001, ****P<0.0001. DEX-HCl, Dexmedetomidine hydrochloride; SFC, sufentanil citrate; MMP2, metalloproteinase 2; MMP9, metalloproteinase 9.

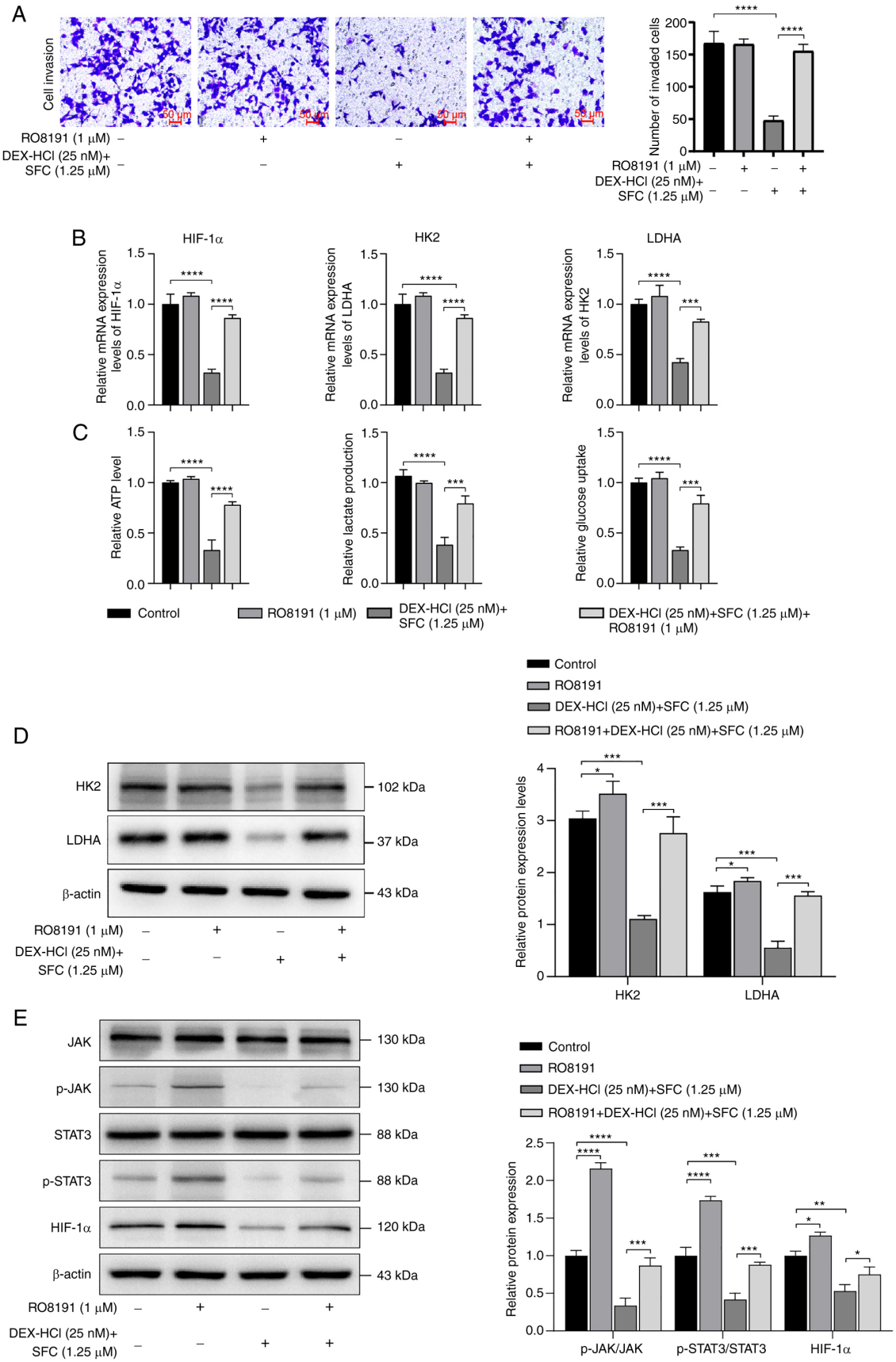

Figure 5. RO8191 counteracts the effects of DEX-HCl combined with SFC on KYSE30 cell invasion, migration and glucose metabolism. (A) Transwell assay to test the effect of RO8191 on the invasion ability of KYSE30 cells treated with DEX-HCl and SFC. (B) RT-qPCR was used to assess changes in relative mRNA expression of HIF-1α, HK2, and LDHA genes in KYSE30 cells. (C) Detection of changes in lactate, glucose and ATP content in KYSE30 cells. (D) Semi-quantified protein expression levels assessed by western blotting of glucose metabolism-related proteins HK2 and LDHA. (E) Semi-quantified protein expression levels assessed by western blotting of p-JAK, p-STAT 3 and HIF-1α proteins. *P<0.05, **P<0.01, ***P<0.001, ****P<0.0001. DEX-HCl, Dexmedetomidine hydrochloride; SFC, sufentanil citrate; HIF-1α, Hypoxia-inducible factor-1α; p-JAK, phosphorylated Janus kinase; p-STAT 3, phosphorylated signal transducer and activator 3; RT-qPCR, reverse transcription-quantitative PCR.

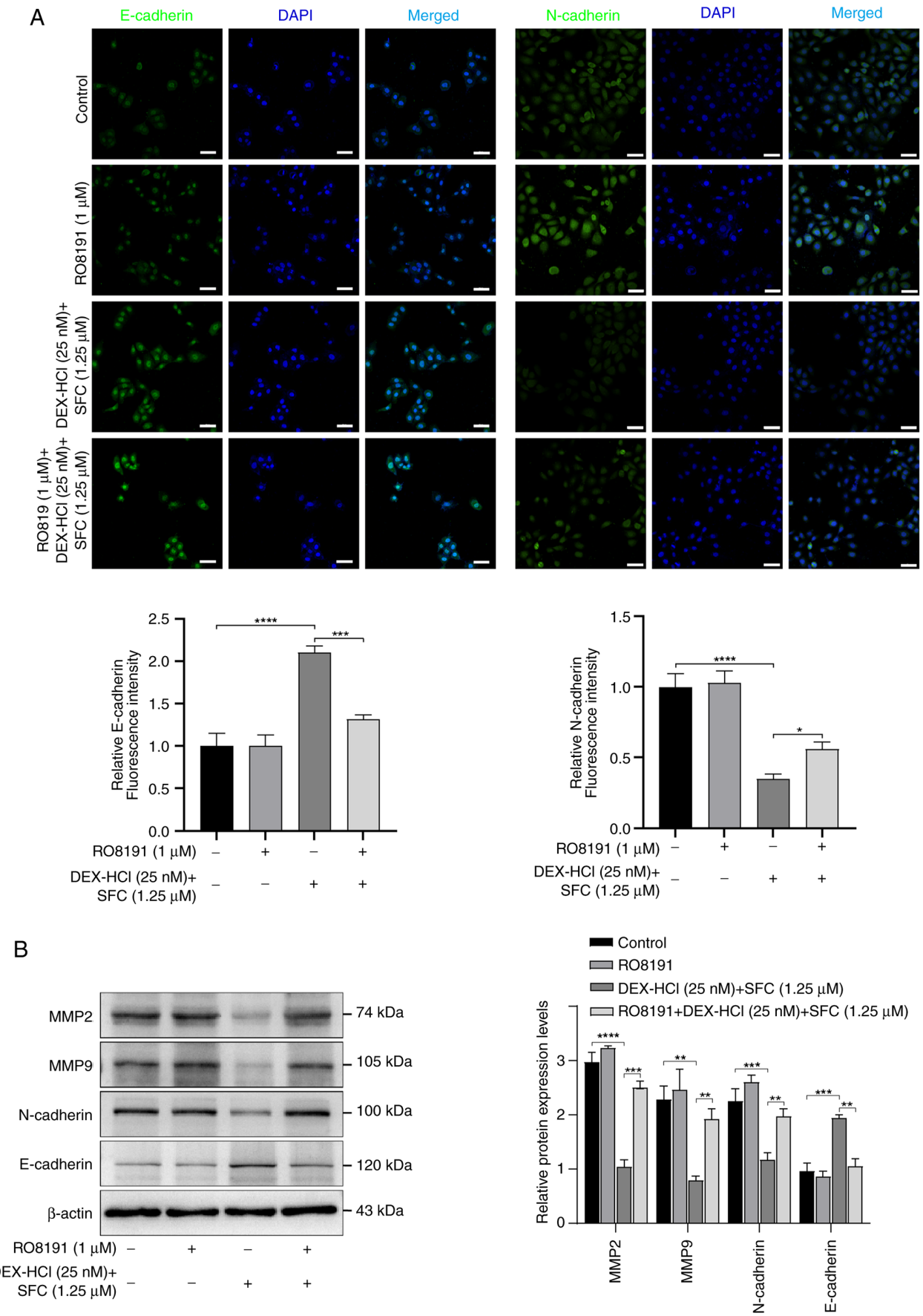

Figure 6. Immunofluorescence and western blotting of invasion-related proteins from KYSE30 cells treated with RO8191 and DEX-HCl and SFC combined treatment. (A) Immunofluorescence images and quantification of N-cadherin and E-cadherin in KYSE30 cells after treatment with RO8191 and DEX-HCl and SFC combined treatment (scale bar, 50 μm). (B) Semi-quantified protein expression levels assessed by western blotting of MMP2, MMP9, E-cadherin, and N-cadherin. *P<0.05, **P<0.01, ***P<0.001, ****P<0.0001. DEX-HCl, Dexmedetomidine hydrochloride; SFC, sufentanil citrate; MMP2, metalloproteinase 2; MMP9, metalloproteinase 9.

in combination with SFC was able to inhibit KEYSE30 cell invasion and inhibit JAK/STAT3/HIF-1α axis activation, and RO8191, as a JAK/STAT3 pathway activator, was able to reverse this effect, which reinforces the conclusion that the inhibitory effect of DEX-HCI in combination with SFC on KEYSE30 cell invasion was mediated by the inhibition of JAK/STAT3/HIF-1α axis activation. STAT3/HIF-1α axis to exert pharmacological effects.

Discussion

A major cause of the current low 5-year survival rate after EC surgery is the epithelial-mesenchymal transition (2). EMT serves a key role in skin injury healing and tumor invasion and metastasis (30), and elevated expression of MMP2 and MMP9 promotes EC proliferation, accelerates the EMT process and facilitates tumor angiogenesis (31). MMP2 and MMP9 are risk factors for metastasis and poor prognosis in EC (32). The results of the present study demonstrated that DEX-HCl and SFC could inhibit the proliferation, invasion and migration of KYSE30 cells and suppress the protein expression levels of MMP2 and MMP9, and that the inhibitory effect was increased following the co-administration of DEX-HCL and SFC. Aberrant expression of N-cadherin and low expression of E-cadherin are important indicators of poor prognosis and EMT in EC (33,34). E-cadherin determines the adhesion ability between epithelial cells during the development of EMT. Dysregulation of E-cadherin protein expression leads to the loss of the adhesion ability of tumor cells and contributes to the metastasis of tumor cells (35). Moreover, previous studies have reported that N-cadherin can induce tumor cell invasion and angiogenesis (36,37), and a number of N-cadherin antagonists have been adopted for tumor therapy (38). The present study demonstrated that DEX-HCl combined with SFC significantly upregulated E-cadherin and significantly downregulated N-cadherin protein expression levels, thereby inhibiting KYSE30 cell metastasis and EMT.

DEX-HCl has been reported to inhibit growth and metastasis (39) and to induce apoptosis in EC cells (40). Previous studies have reported that SFC could also inhibit EC cell metastasis (41), which was consistent with the findings of this study. However, neither elaborated on the effects of co-administration of DEX-HCl and SFC on glucose metabolism in EC cells. Cancer cells require substantial amounts of energy during metastasis, which is supplied directly through the glycolytic pathway (42). The preferred metabolic pathway in cancer cells under aerobic conditions is glycolysis for energy supply rather than oxidative phosphorylation, a phenomenon known as the Warburg effect (43). Therefore, inhibition of tumor glycolysis is considered a new strategy to inhibit tumor proliferation and metastasis (44). The results of the current study indicated that DEX-HCl and SFC treatments reduced ATP production and cellular glucose metabolism in KYSE30 cells. Furthermore, co-administration of DEX-HCl and SFC enhanced their individual inhibitory effects on proliferation, migration and invasion of KYSE30 cells, as well as increasing the reduction in ATP production and glucose metabolism in KYSE30 cells compared with single treatment. Furthermore, overexpression of LDHA in tumor cells has been frequently reported (45,46). In addition to promoting glycolysis, elevated LDHA levels in tumors also facilitates lactate production, thereby reconstituting the tumor microenvironment and inhibiting the immune system to promote immune escape (47). DEX-HCl and SFC can decrease lactate production and downregulate mRNA and protein expression levels of HK2 and LDHA, thereby suppressing KYSE30 cell invasive migration.

The present study demonstrated that DEX-HCl combined with SFC inhibited KYSE30 cell invasion and metastasis and blocked KYSE30 cell glucose metabolism. Moreover, previous studies have reported that JAK and STAT3 are involved in all stages of development from cancer cell proliferation to cancer cell metastasis (48,49). In rheumatoid arthritis, JAK/STAT3 exerts anti-inflammatory effects by regulating HIF-1α expression (50), CXCL8 promotes melanoma progression by activating the JAK/STAT1/HIF-1α axis (51), and ELTD1 promotes glioma proliferation, migration and invasion by activating the JAK/STAT3/HIF-1α signaling axis (52). Therefore, this pathway may be a potential target for inhibiting the metastasis of cancer cells. The present study demonstrated that DEX-HCl combined with SFC inhibited the JAK/STAT1/HIF-1α axis and suppressed KYSE30 cell metastasis and glucose metabolism, and that the inhibitory effect was counteracted by the addition of RO8191, which activated the phosphorylation of JAK and STAT proteins which increased the protein expression levels of MMP2, MMP9, N-cadherin and E-cadherin, suggesting the results of DEX-HCl and SFC treatment involve the modulation of the JAK/STAT signaling pathway. Furthermore, *in vitro* experiments demonstrated that DEX-HCl and SFC may regulate glucose metabolism-related indicators through the JAK/STAT3/HIF-1α axis, thereby inhibiting KYSE30 cell invasion and migration. However, further studies are required to elucidate the in-depth mechanism by which DEX-HCl combined with SFC affects glucose metabolism in KYSE30 cells.

In the present study, DEX-HCl and SFC were demonstrated to decrease the expression of EC and metastasis-related proteins, significantly reducing glucose uptake, ATP and lactate production in KYSE30 cells. The pharmacological effects were significantly enhanced by the combined action of DEX-HCI and SFC, and reverse validation experiments with RO8191 confirmed the possible involvement of the JAK/STAT3/HIF-1α axis in this process.

Acknowledgments

Not applicable.

Funding

This work was supported by the Natural Science Foundation of Hebei Province (grant no. H2020206397).

Availability of data and materials

The datasets used and/or analyzed during the current study are available from the corresponding author on reasonable request.

Authors' contributions

WL, YW, XL, HW and LJ were involved in the design of the project. WL wrote the first draft of the article. HW was

responsible for the final revision and layout of the article. XL was responsible for the literature search and experimental methods. YW was responsible for conducting the experiments. LJ was responsible for the data processing and general notation series. WL and YW confirm the authenticity of all the raw data. All authors read and approved the final version of the manuscript.

Ethics approval and consent to participate

Not applicable.

Patient consent for publication

Not applicable.

Competing interests

The authors declare that they have no competing interests.

References

1. Liu CQ, Ma YL, Qin Q, Wang PH, Luo Y, Xu PF and Cui Y: Epidemiology of esophageal cancer in 2020 and projections to 2030 and 2040. Thorac Cancer 14: 3-11, 2023.
2. Liu Z, Zhao Y, Kong P, Liu Y, Huang J, Xu E, Wei W, Li G, Cheng X, Xue L, *et al*: Integrated multi-omics profiling yields a clinically relevant molecular classification for esophageal squamous cell carcinoma. Cancer Cell 41: 181-195, 2023.
3. Morgan E, Soerjomataram I, Rumgay H, Coleman HG, Thrift AP, Vignat J, Laversanne M, Ferlay J and Arnold M: The global landscape of esophageal squamous cell carcinoma and esophageal adenocarcinoma incidence and mortality in 2020 and projections to 2040: New estimates from GLOBOCAN 2020. Gastroenterology 163: 649-658, 2022.
4. Li P, Jing J, Liu W, Wang J, Qi X and Zhang G: Spatiotemporal patterns of esophageal cancer burden attributable to behavioral, metabolic, and dietary risk factors from 1990 to 2019: Longitudinal observational study. JMIR Public Health Surveill 9: e46051, 2023.
5. Codipilly DC and Wang KK: Squamous cell carcinoma of the esophagus. Gastroenterol Clin North Am 51: 457-484, 2022.
6. Lu D, Wu X, Wu W, Wu S, Li H, Zhang Y, Yan X, Zhai J, Dong X, Feng S, *et al*: Plasma cell-free DNA 5-hydroxymethylcytosine and whole-genome sequencing signatures for early detection of esophageal cancer. Cell Death Dis 14: 843, 2023
7. Wang S, Zheng R, Arnold M, Abnet C, Zeng H, Zhang S, Chen R, Sun K, Li L, An L, *et al*: Global and national trends in the age-specific sex ratio of esophageal cancer and gastric cancer by subtype. Int J Cancer 151: 1447-1461, 2022.
8. Manfioletti G and Fedele M: Epithelial-mesenchymal transition (EMT). Int J Mol Sci 24: 11386, 2023
9. Lu W and Kang Y. Epithelial-mesenchymal plasticity in cancer progression and metastasis. Dev Cell 49: 361-374, 2019.
10. Counihan JL, Grossman EA and Nomura DK: Cancer metabolism: Current understanding and therapies. Chem Rev 118: 6893-6923, 2018.
11. Zhang M, Wei T, Zhang X and Guo D: Targeting lipid metabolism reprogramming of immunocytes in response to the tumor microenvironment stressor: A potential approach for tumor therapy. Front Immunol 13: 937406, 2022.
12. Xin P, Xu X, Deng C, Liu S, Wang Y, Zhou X, Ma H, Wei D and Sun S: The role of JAK/STAT signaling pathway and its inhibitors in diseases. Int Immunopharmacol 80: 106210, 2020.
13. Zhang P, Li Z and Yang G: Silencing of ISLR inhibits tumour progression and glycolysis by inactivating the IL-6/JAK/STAT3 pathway in non-small cell lung cancer. Int J Mol Med 48: 222, 2021.
14. Xiao C, Zhang W, Hua M, Chen H, Yang B, Wang Y and Yang Q: RNF7 inhibits apoptosis and sunitinib sensitivity and promotes glycolysis in renal cell carcinoma via the SOCS1/JAK/STAT3 feedback loop. Cell Mol Biol Lett 27: 36, 2022.
15. Lei K, Du W, Lin S, Yang L, Xu Y, Gao Y, Xu B, Tan S, Xu Y, Qian X, *et al*: 3B, a novel photosensitizer, inhibits glycolysis and inflammation via miR-155-5p and breaks the JAK/STAT3/SOCS1 feedback loop in human breast cancer cells. Biomed Pharmacother 82: 141-150, 2016.
16. You Z, Xu D, Ji J, Guo W, Zhu W and He J: JAK/STAT signal pathway activation promotes progression and survival of human oesophageal squamous cell carcinoma. Clin Transl Oncol 14: 143-149, 2012.
17. Zhao X, Tang YP, Wang CY, Wu JX and Ye F: Prognostic values of STAT3 and HIF-1lα in esophageal squamous cell carcinoma. Eur Rev Med Pharmacol Sci 23: 3351-3357, 2019.
18. Fang J, Chu L, Li C, Chen Y, Hu F, Zhang X, Zhao H, Liu Z and Xu Q: JAK2 inhibitor blocks the inflammation and growth of esophageal squamous cell carcinoma in vitro through the JAK/STAT3 pathway. Oncol Rep 33: 494-502, 2015.
19. Yang Y, Jin G, Liu H, Liu K, Zhao J, Chen X, Wang D, Bai R, Li X, Jang Y, *et al*: Metformin inhibits esophageal squamous cell carcinoma-induced angiogenesis by suppressing JAK/STAT3 signaling pathway. Oncotarget 8: 74673-74687, 2017.
20. Garcia SN, Guedes RC and Marques MM: Unlocking the potential of HK2 in cancer metabolism and therapeutics. Curr Med Chem 26: 7285-7322, 2019.
21. Zhang L, Jiang C, Zhong Y, Sun K, Jing H, Song J, Xie J, Zhou Y, Tian M, Zhang C, *et al*: STING is a cell-intrinsic metabolic checkpoint restricting aerobic glycolysis by targeting HK2. Nat Cell Biol 25: 1208-1222, 2023.
22. Xun S and Zheng R: Dexmedetomidine alleviates neuropathic pain by regulating JAK/STAT pathway in rats. J Cell Biochem 121: 2277-2283, 2020.
23. Si Y, Bao H, Han L, Shi H, Zhang Y, Xu L, Liu C, Wang J, Yang X, Vohra A and Ma D: Dexmedetomidine protects against renal ischemia and reperfusion injury by inhibiting the JAK/STAT signaling activation. J Transl Med 11: 141, 2013.
24. Zhang Y, Jiang W and Luo X: Remifentanil combined with dexmedetomidine on the analgesic effect of breast cancer patients undergoing modified radical mastectomy and the influence of perioperative T lymphocyte subsets. Front Surg 9: 1016690, 2022.
25. Cai Q, Liu G, Huang L, Guan Y, Wei H, Dou Z, Liu D, Hu Y and Gao M: The role of dexmedetomidine in tumor-progressive factors in the perioperative period and cancer recurrence: A narrative review. Drug Des Devel Ther 16: 2161-2175, 2022.
26. Zhang H, Qu M, Guo K, Wang Y, Gu J, Wu H, Zhu X, Sun Z, Cata JP, Chen W and Miao C: Intraoperative lidocaine infusion in patients undergoing pancreatectomy for pancreatic cancer: A mechanistic, multicentre randomised clinical trial. Br J Anaesth 129: 244-253, 2022.
27. Ruijter JM, Barnewall RJ, Marsh IB, Szentirmay AN, Quinn JC, van Houdt R, Gunst QD and van den Hoff MJB: Efficiency correction is required for accurate quantitative PCR analysis and reporting. Clin Chem 67: 829-842, 2021.
28. Chou TC: Drug combination studies and their synergy quantification using the Chou-Talalay method. Cancer Res 70: 440-446, 2010.
29. Meng J, Zhang C, Zhu N, Zhang C, Liu M, Han Z and Li Y: EPN3 plays oncogenic role in non-small cell lung cancer by activating the JAK1/2-STAT3 pathway. Environ Toxicol 38: 1968-1979, 2023.
30. Gundamaraju R, Lu W, Paul MK, Jha NK, Gupta PK, Ojha S, Chattopadhyay I, Rao PV and Ghavami S: Autophagy and EMT in cancer and metastasis: Who controls whom?. Biochim Biophys Acta Mol Basis Dis 1868: 166431, 2022.
31. Zhang X, Shi G, Gao F, Liu P, Wang H and Tan X: TSPAN1 upregulates MMP2 to promote pancreatic cancer cell migration and invasion via PLCγ. Oncol Rep 41: 2117-2125, 2019.
32. Zhang L, Xi RX and Zhang XZ: Matrix metalloproteinase variants associated with risk and clinical outcome of esophageal cancer. Genet Mol Res 14: 4616-4624, 2015.
33. Xu XL, Ling ZQ, Chen SZ, Li B, Ji WH and Mao WM: The impact of E-cadherin expression on the prognosis of esophageal cancer: A meta-analysis. Dis Esophagus 27: 79-86, 2014.
34. Zhu S, Liu J, Min L, Sun X, Guo Q, Li H, Zhang Z, Zhao Y, Gu J and Zhang S: Cadherin expression shift could well distinguish esophageal squamous cell carcinoma from non- cancerous esophageal tissues. Oncol Res Treat 41: 380-385, 2018.
35. Mendonsa AM, Na TY and Gumbiner BM: E-cadherin in contact inhibition and cancer. Oncogene 37: 4769-4780, 2018.
36. Parker J, Hockney S, Blaschuk OW and Pal D: Targeting N-cadherin (CDH2) and the malignant bone marrow microenvironment in acute leukaemia. Expert Rev Mol Med 25: e16, 2023.
37. Lou C, Wu K, Shi J, Dai Z and Xu Q: N-cadherin protects oral cancer cells from NK cell killing in the circulation by inducing NK cell functional exhaustion via the KLRG1 receptor. J Immunother Cancer 10: e005061, 2022.

38. Mariotti A, Perotti A, Sessa C and Rüegg C: N-cadherin as a therapeutic target in cancer. Expert Opin Investig Drugs 16: 451-465, 2007.
39. Yoshio T, Ishiyama A, Tsuchida T, Yoshimizu S, Horiuchi Y, Omae M, Hirasawa T, Yamamoto Y, Sano H, Yokota M and Fujisaki J: Efficacy of novel sedation using the combination of dexmedetomidine and midazolam during endoscopic submucosal dissection for esophageal squamous cell carcinoma. Esophagus 16: 285-291, 2019.
40. Che J, Liu M and Lv H: Dexmedetomidine disrupts esophagus cancer tumorigenesis by modulating circ_0003340/miR-198/HMGA2 axis. Anticancer Drugs 33: 448-458, 2022.
41. Tang H, Li C, Wang Y and Deng L: Sufentanil inhibits the proliferation and metastasis of esophageal cancer by inhibiting the NF-κB and snail signaling pathways. J Oncol 2021: 7586100, 2021.
42. Kocianova E, Piatrikova V and Golias T: Revisiting the warburg effect with focus on lactate. Cancers (Basel) 14: 6028, 2022.
43. Zhong X, He X, Wang Y, Hu Z, Huang H, Zhao S, Wei P and Li D: Warburg effect in colorectal cancer: The emerging roles in tumor microenvironment and therapeutic implications. J Hematol Oncol 15: 160, 2022.
44. Chelakkot C, Chelakkot VS, Shin Y and Song K: Modulating glycolysis to improve cancer therapy. Int J Mol Sci 24: 2606, 2023.
45. Zhang K, Zhang T, Yang Y, Tu W, Huang H, Wang Y, Chen Y, Pan K and Chen Z: N(6)-methyladenosine-mediated LDHA induction potentiates chemoresistance of colorectal cancer cells through metabolic reprogramming. Theranostics 12: 4802-4817, 2022.
46. Jacquet P and Stephanou A: Searching for the metabolic signature of cancer: A review from warburg's time to now. Biomolecules 12: 1412, 2022.
47. Brand A, Singer K, Koehl GE, Kolitzus M, Schoenhammer G, Thiel A, Matos C, Bruss C, Klobuch S, Peter K, *et al*: LDHA-associated lactic acid production blunts tumor immunosurveillance by T and NK cells. Cell Metab 24: 657-671, 2016.
48. Dinakar YH, Kumar H, Mudavath SL, Jain R, Ajmeer R and Jain V: Role of STAT3 in the initiation, progression, proliferation and metastasis of breast cancer and strategies to deliver JAK and STAT3 inhibitors. Life Sci 309: 120996, 2022.
49. Malekan M, Ebrahimzadeh MA and Sheida F: The role of Hypoxia-Inducible Factor-1alpha and its signaling in melanoma. Biomed Pharmacother 141: 111873, 2021.
50. Hu L, Liu R and Zhang L: Advance in bone destruction participated by JAK/STAT in rheumatoid arthritis and therapeutic effect of JAK/STAT inhibitors. Int Immunopharmacol 111: 109095, 2022.
51. Hu X, Yuan L and Ma T: Mechanisms of JAK-STAT signaling pathway mediated by CXCL8 gene silencing on epithelial-mesenchymal transition of human cutaneous melanoma cells. Oncol Lett 20: 1973-1981, 2020.
52. Li J, Shen J, Wang Z, Xu H, Wang Q, Chai S, Fu P, Huang T, Anas O, Zhao H, *et al*: ELTD1 facilitates glioma proliferation, migration and invasion by activating JAK/STAT3/HIF-1alpha signaling axis. Sci Rep 9: 13904, 2019.